

NUMERICAL ANALYSIS OF THE REINFORCED RETAINING WALL ON YIELDING OR ON NON-YIELDING FOUNDATION SOIL

Mica Lumir¹, Racansky Vaclav² & Petr Klablana³

¹ Brno University of Technology, Faculty of Civil Engineering, Czech Republic. (e-mail: mica.l@fce.vutbr.cz)

² Brno University of Technology, Faculty of Civil Engineering, Czech Republic. (e-mail: racansky.v@fce.vutbr.cz)

³ Geotechnika spol. s r.o., Kotlarska 24, 60200 Brno, Czech Republic. (e-mail: geotechnika@seznam.cz)

Abstract: Conventional methods like limit equilibrium method are most often used for design of reinforced retaining walls. These methods assume that the soil is at failure and the failure mechanism is known. The soil stiffness is excluded from analyses of these type. The paper shows an influence of the stiffness of the foundation soil on the behaviour of the earth reinforced retaining wall. The geosynthetic-reinforced segmental retaining wall and a full height panel face wall tied back by geosynthetics is modelled. The first type of wall is used frequently in the Czech Republic. Parametric numerical study is performed by means of the finite element analysis. For geosynthetics, elastoplastic elements defined by the axial stiffness "EA" and the allowable tensile strength "N_p" are used. Hardening soil model (HS) and soft soil model (S-S) are used for modelling of the soil behaviour. The outcome of this numerical study is better understanding of the behaviour of such a structure (e.g. deformation of the face, force redistribution in the reinforcement).

Keywords: Soil reinforcement, reinforced earth retaining wall, segmental retaining wall, geogrid reinforcement, geotechnical design, finite element.

INTRODUCTION

After the initial distrust, reinforced retaining walls are becoming more and more popular in the Czech Republic. They are often used as a replacement for conventional retaining structures or for structures like bridge abutments, etc. Walls with face panels made of gravity stones or "T" shaped panels with retaining heights over 10 m are not uncommon practice nowadays.

Software packages based on the limit equilibrium analysis are used for design of such walls. Design checks concern overall and internal stability of the structure. Overall stability design check assumes that the reinforced soil wall behaves essentially as a rigid body and conforms to the simple laws of statics.

The internal stability is essentially associated with the tension and pullout failure mechanisms of the reinforcement. The designer must ensure that neither of these failure mechanisms is allowed to occur by investigating the internal behaviour mechanisms and stress patterns within the structure. The Tie-back Wedge Method is most widely used to analyse the internal stability of reinforced soil wall. Input parameters for this design are: friction angle (ϕ'/ϕ_u), cohesion (c'/c_u) and weight of soil (γ/γ_{sat}). The stiffness parameters are not included in this type of design. Design procedure cannot take deformation parameters and its influences on internal stresses into account.

More advanced calculation methods as finite element method or finite difference method may be used in order to examine stresses and displacements. A finite element method is used throughout this analysis. This topic was treated by several authors as Rowe & Skinner (2001), Skinner & Rowe (2005) and Yoo & Song (2006), as well using FEM for analysing the problem.

Results from these studies show that the stiffness of the foundation soil have an effect on the behaviour of the reinforced soil wall (especially on the Geosynthetic-reinforced segmental walls (GR-SRWs)). Authors (Skinner and Rowe 2005) focused on the effect of the bottom reinforcement layer on the bearing capacity of the GR-SRWs in soft clays. Yoo and Song (2006) investigated the yielding effect of two-tiered GR-SRWs in sands.

This paper is concentrating on the examination of effects of different overconsolidation levels on the behaviour of the GR-SRWs and geosynthetic-reinforced full high panel retaining walls (GR- FHPRWs).

Soil conditions for the analysis were chosen to represent typical soil profile (Miocene clays) of Brno (city) and the Moravia region.

MIOCENE CLAYS

Brno clay constitutes subsoil in most areas of Brno and its surroundings. These are highly calcareous clays, which can be locally classified as silty clays. Predominantly, they do not possess layered structure, but slight layering might occur occasionally. They date back to the Miocene Epoch (13 millions years old). Clays are found in layers of up to 200 m of thickness. Sometimes, inclusions of coarse grained material are found in the clay, which can cause strong inflows if found during excavation works.

The preconsolidation of clays is not very high as glaciation never extended over the Brno region. The pre-overburden pressure is estimated somewhere between 100 – 600 kPa. Brno clays are often fissured. Soil properties, as described by (Horák, 1987):

- Soil properties – unit weight $\rho = 1895 \text{ kg.m}^{-3}$, dry unit weight $\rho_d = 1440 \text{ kg.m}^{-3}$, specific weight $\rho_s = 2665 \text{ kg.m}^{-3}$, liquidity limit $w_{LL} = 78.5\%$, plasticity limit $w_{PL} = 36.6\%$, saturation ratio $S_r = 96\div 100\%$, permeability $k = 7 \times 10^{-10} \text{ m.s}^{-1}$.

- Stiffness – stress range (0.4 – 0.8) MPa Edometric modul $E_o' = (15 – 20)$ MPa. Other author, Boháč (1995, 1999) shown that initial modulus determined from hyperbolic transformation is from 30 MPa to 80 MPa.
- Strength – peak strength - $\phi_p' = 20^\circ \div 22^\circ$ (exceptionally 28°), cohesion $c_p' = 20$ kPa \div 100 kPa for depths of 20 – 30 m (shear box test). Results of another test series give $\phi_p' = 28,5^\circ$, $c_p' = 18$ kPa up to depths of 20m. For samples (depths of 22 m) $\phi_p' = 27,6^\circ$, $c_p' = 184$ kPa were measured. Given values were measured in stress range $s' = 100 \sim 550$ kPa where $s' = (\sigma_a' - \sigma_r')/2$ in CIUP triaxial test Boháč (1999).

Above given parameters are based on different sources. The clays were also tested at our Institute laboratory at Brno University of Technology by Uhrin (2004) and Erbenová (2006) on reconstituted samples from depth of 12 and 24 m. Soil parameters used in FE analysis are listed in part 3.2.

MUMERICAL MODEL

Description of model

The geometry of an embankment and placement of the reinforcement for GR-SRW and GR-FHPRW considered in this study is shown in Figure 1. The model is using symmetry, therefore only half of the embankment is modelled.

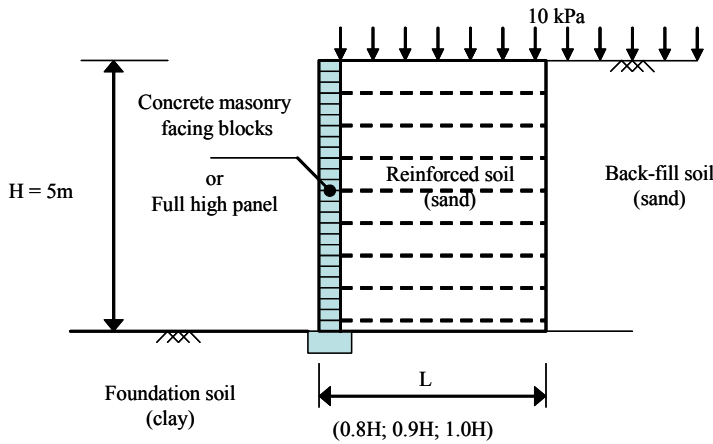


Figure 1. Geometry used for the analysis (cross-section)

The reinforcement type (stiffness “EA” and allowable tensile strength “ N_p ”), length ($L_{basic} = 0.9H$) and its distribution was determined from the software WinWall ver. 8, module “Tensor Tie-back Wedge design” where strength parameters (ϕ'_{cv} and c'_{cv}) are used as inputs (Penman, 1998). Design of the reinforcement was done for the GR-SRW. The same design was applied to GR-FHPW, however when using full height panel retaining wall, the spacing of reinforcement may be usually higher then for segmental walls.

The type of wall face as well as the length of base were varied for different calculations according to Table 1.

Table 1. Cases analysed

Face type	L (times H)	POP* (kPa)
Blocks (450x300x190mm)	0.8H; 0.9H; 1.0H	50; 100; 600
Full high panel	0.8H; 0.9H; 1.0H	50; 100; 600

* pre-overburden pressure

FE code PLAXIS V8.4 (Vermeer, T. & Brinkgreve, R.B.J., 1998) was used for calculations. A 2D plane strain analysis (width of the model is 65 m and the depth is 20 m) was used. The FE mesh (Figure 2.) consists of 8407 six-noded triangular elements used to model the soil and the concrete face behaviour. Geosynthetics are modelled as line elements with axial stiffness and no bending stiffness. Elastoplastic behaviour is assigned to these elements by defining the axial stiffness “EA” and the allowable tensile strength “ N_p ”. Drained soil behaviour is considered in the analysis, as a long term behaviour of the structure is of an interest. There are no interface elements used around the geogrid, since a full contact between soil and a geogrid is assumed in the analysis. A reduced stiffness was used for face panels of geosynthetic-reinforced segmental wall ($E = 1.0$ GPa) in order to consider the fact, that the wall consists of segments. Same approach is adopted in paper of Yoo and Song (2006). Varying overconsolidation level which causes different soil stiffnesses was modelled by using pre-overburden pressure (POP) (Plaxis, 2004), which is defined as:

$$POP = |\sigma'_p - \sigma'_{yy}|$$

Where σ_p is pre-consolidation stress in kPa and σ'_{yy} is in-situ effective vertical stress in kPa. The construction sequence was modelled in 2 construction stages. In the first stage, the initial stresses were generated and in the second, the structure and the load of 10 kPa were activated.

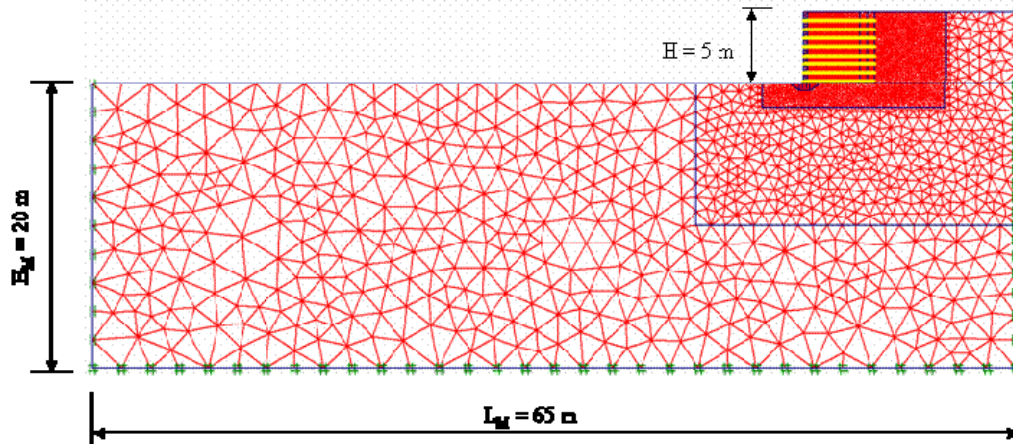


Figure 2. Finite element mesh for an analysis GR-SRW and GR-FHPRW.

Input data

The subsoil (Miocene Clay) was modelled with Soft-Soil model (S-S). S-S model is an elastoplastic model which assumes stress dependent stiffness (logarithmic compression behaviour), distinction between primary loading and unloading-reloading, memory for the pre-consolidation stress and failure behaviour according to the Mohr-Coulomb criterion. Parameters for the S-S model were determined from laboratory tests ($\lambda = 0.259$, $\kappa = 0.0518$). The reinforced soil and the backfill (sand) was modelled with the Hardenig soil (HS) model. The HS model is a double hardening elastoplastic model incorporating deviatoric and volumetric hardening. For deviatoric hardening a non-associated flow rule and for the volumetric hardening an associated flow rule is assumed (Schanz, Vermeer and Bonnier, 1999). The main features of the model are stress dependent stiffness according to the power law, distinction between primary loading and unloading-reloading, memory for the pre-consolidation stress and failure behaviour according to the Mohr-Coulomb criterion.

The parameters for HS model were taken from literature (Vermeer, T. & Brinkgreve, R.B.J., 1998). The parameters used in the numerical analysis are listed in the Table 2.

Table 2. Model parameters for foundation, reinforced and back fill soil

soil parameter	Un it	S-S constitutive model (foundation soil)	HS constitutive model (reinforced/back-fill)
γ_{unsat}	kN.m^{-3}	19.0	17.0
γ_{sat}	kN.m^{-3}	21.0	17.0
$k_x = k_y$	m.s^{-1}	1e-10	1e-10
E_{50}^{ref}	MPa	-	30.0
$E_{\text{oed}}^{\text{ref}}$	MPa	-	30.0
$E_{\text{ur}}^{\text{ef}}$	MPa	-	90.0
λ^*	-	0.07	-
κ^*	-	0.014	-
c'_{cv}	kPa	0	0
ϕ'_{cv}	°	27.7	35
v_{ur}	-	0.15	0.2
m	-	-	0.5
R_f	-	-	0.9
ρ_{ref}	kPa	-	100

The input data for geogrid and concrete structures are in Table 3 and Table 4. For the wall face behaviour identical elements as for the soil modelling were used. Elastic behaviour was assigned to them.

Table 3. Model parameters for the concrete structures

Parameter	Unit	GR-SRW	GR-FHPW
E	GPa	1.0	25
ν	-	0.15	0.15

Table 4. Model parameters for geogrid

parameter	Unit	GR-SRW	GR-FHPW
EA	kN/m	635	635
N_p	kN/m	12.7	12.7

RESULTS AND DISCUSSION

All cases given in Table 1 were analysed. Performance of modelled structures is discussed with respect to displacements and axial forces generated in the reinforcement.

Displacements

Maximal settlements of centre of the embankment for different variants are: POP = 50 kPa → $s = 350$ mm; POP = 100 kPa → $s = 110$ mm a POP = 600 kPa → $s = 82$ mm. The average base inclination sloping towards the centre of the embankment is 0.03%, 0.007% and 0.006% for POP = 50 kPa, 100 kPa and 600 kPa respectively. The influence of different face types on calculated settlements was negligible in all cases. One can notice a great difference in settlements as well as in the base inclination for the case of 50 kPa of pre-overburden pressure of and 100 kPa. Much less pronounced difference is calculated between 100 and 600 kPa.

This is not a surprise and the behaviour can be explained when comparing the pre-overburden pressure with the total load of the embankment. The total load applied on the base of the embankment is approx. 95 kPa. Thus for POP of 50 kPa, the loading is initially below the level of overconsolidation where the unloading-reloading stiffness is being used. Once the load exceeds the POP, the constitutive model switches to the initial loading stiffness automatically. On the other hand, for higher levels of overconsolidation is our loading path always below POP and thus the model is using the unloading-reloading stiffness only. As the unloading-reloading stiffness is approx. five times higher than the initial loading one, is it easy to understand why are the settlements of the embankment significantly higher for case of POP = 50 kPa.

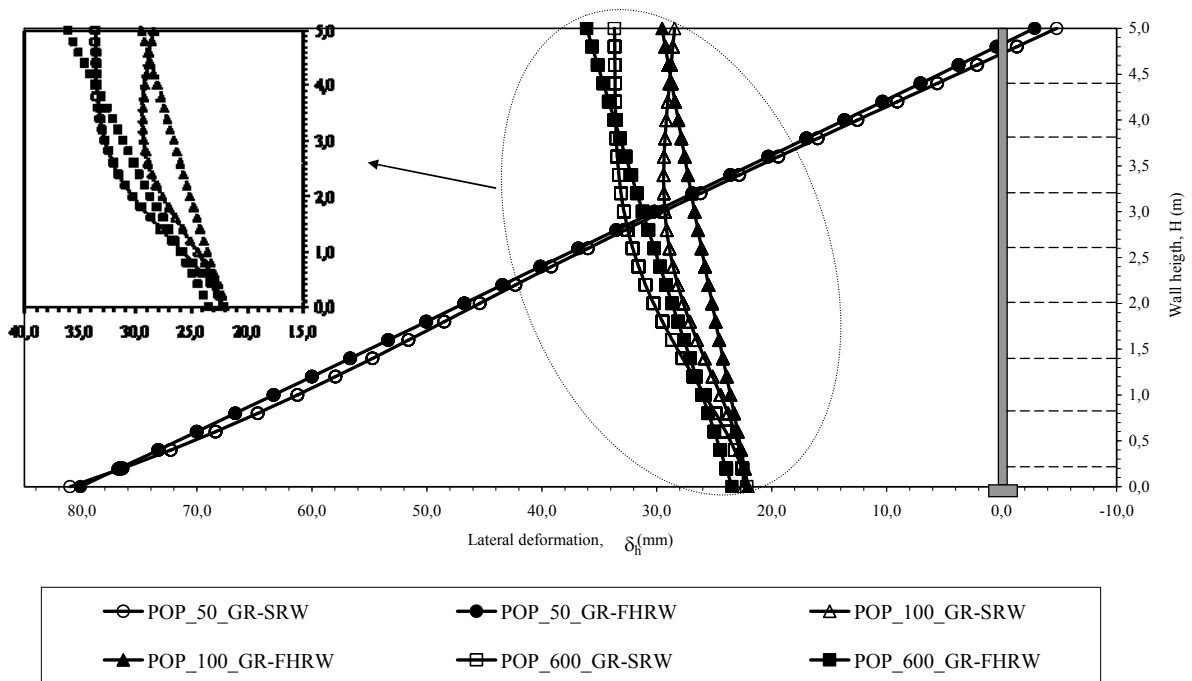


Figure 3. Lateral deformation of wall for different cases

Horizontal wall displacements are influenced by different stiffnesses of the subsoil. Again for POP of 50 kPa, the subsoil behaves much softer than for other two cases. Horizontal wall displacements of analysed structures are shown in Figure 3 and the maximal values are listed in Table 5. For POP of 50 kPa, the subsoil yields to sides due to the added load. Thus the wall rotates clockwise in this case. For stiffer subsoil (POP = 100 kPa and 600 kPa) is the yielding of the wall base overruled by horizontal displacements induced by the earth pressure acting on the back of the wall. Therefore the wall rotates anti-clockwise.

The maximal horizontal displacements of the full-height panel wall are 5÷13% higher than those of the segment wall in the case of POP = 600 kPa, whereas for cases of POP = 50 kPa and 100 kPa were the maximal horizontal displacements nearly identical.

For sake of simplicity, the results are presented for case of $L = 0.9H$ only. For other lengths of reinforcement, the calculated results are similar.

Table 5. Maximal horizontal displacements for $L = 0.9H$

POP	$\delta_{h,max}$ (mm)	
	GR-SRW	GR-FHPW
50	81	80
100	29	29
600	33	36

The segment wall (GR-SRW) shows deflection of the wall face, as the bending stiffness of the face is reduced in this case. The face of the GR-FHPW stayed planar during the whole calculation.

Axial force in the geogrid

Axial forces in the geogrids were compared with respect to different stiffness of the subsoil and to the type of the wall face. Results are shown in Figure 4. Higher axial forces are activated for case of the structure on the softer (yielding) subsoil. With increasing stiffness are the activated axial forces decreasing. Significant difference in axial forces may be noticed among calculations with POP = 50 kPa and 100 kPa. For case of POP = 100 kPa and 600 kPa are axial forces nearly identical.

The type of the wall face has a little influence on axial forces in the geogrid. The magnitude of the force is dependent on the horizontal displacement of the wall. Therefore, the axial forces for GR-SRW are on average by 6% higher than for GR-FHPW. Exceptional are upper two layers of reinforcement where the matter is the other way around. Forces in the geogrid for GR-FHPW are by 3% higher than for GR-SRW. Axial forces in are for all cases lower than the maximal allowable tensile force which defines the onset of the plastic behaviour of the geogrid.

It must be pointed out that the segmented wall was modelled as continuous wall with the reduced stiffness. This simplification is probably causing nearly identical forces for both types of the wall faces. An attempt to model each block separately, which would improve the quality of the model, was not yet successfully resolved.

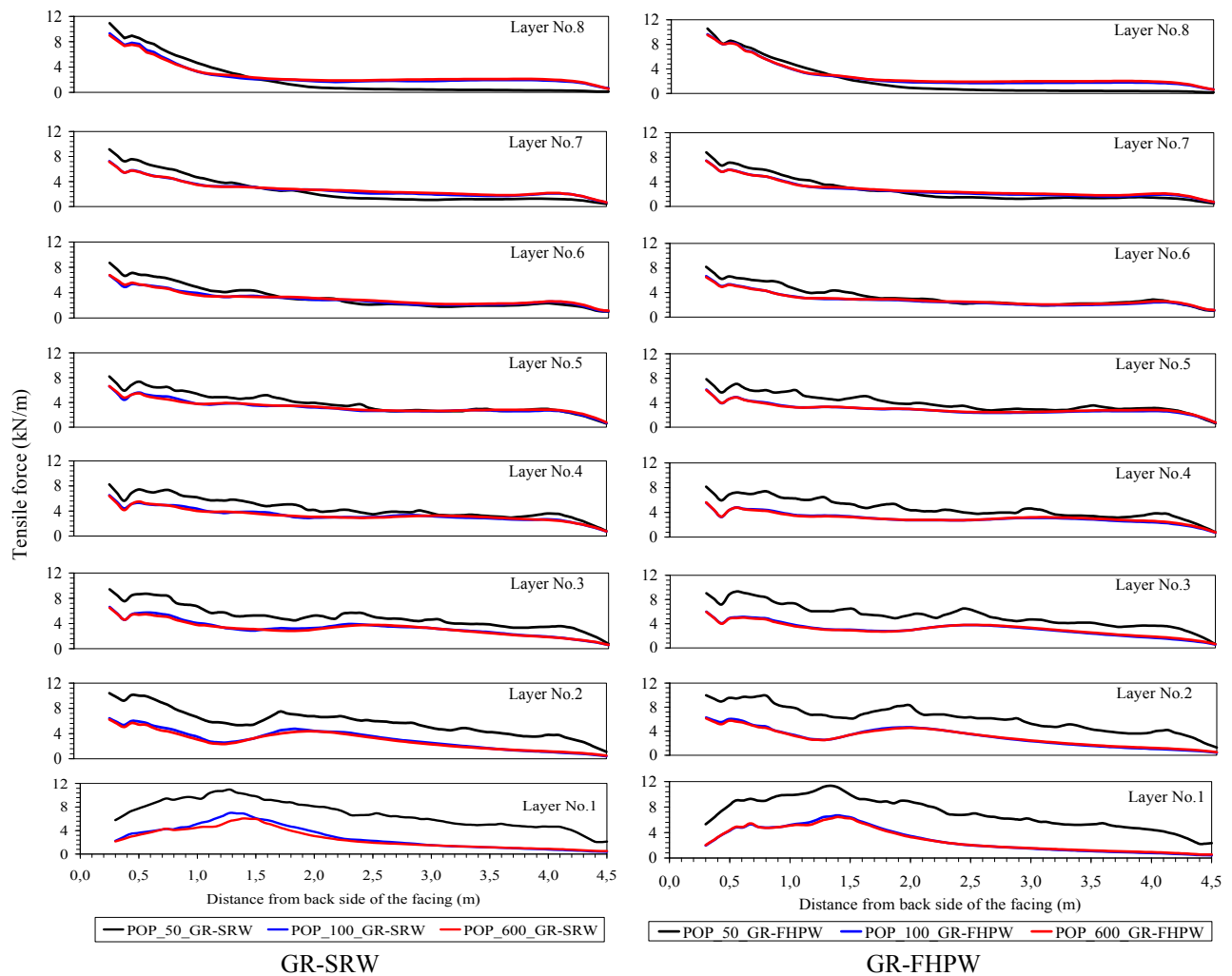


Figure 4. Axial forces for analysed types of walls

CONCLUSIONS

An FE-analysis in order to evaluate the behaviour of the wall on yielding and non-yielding foundation soil was presented. Different levels of over-consolidation resulting in different stiffnesses of subsoil were applied in the study. Two wall face types, namely segmental wall and full high panel retaining wall, were examined.

Horizontal displacements of the wall face were qualitatively different for the soft subsoil, where the wall was laterally displaced and rotated around its top. For the stiffer subsoil, the wall was laterally displaced and rotated around its base. The influence of the type of the wall face on lateral displacements was noticeable for stiffer subsoil conditions only. Maximal displacements were obtained for full high panel retaining wall.

Significantly higher axial forces were obtained for soft subsoil. For higher pre-overburden pressures ($POP \geq 100$ kPa), were differences in geogrid axial forces negligible. Axial forces were independent of the type of the wall face.

The clear influence of the subsoil conditions on axial geogrid forces was shown. However, when neglecting this fact in the conventional design method, acceptable results are obtained as the conventional analysis give generally very conservative design. The fact that tension forces in the geogrid obtained by FE analysis never exceeded forces calculated by conventional design method are proof for this statement.

The analysis was performed for a few geometry arrangements. Tendencies shown here are in agreement with expectations. Further analysis on order to confirm these findings are being done.

Acknowledgements: The article was processed under financial support of the Research Funds MSM0021630519.

Corresponding author: Dr. Lumir Mica, Brno University of Technology, Faculty of Civil Engineering, Department of Geotechnics, Veveri 95, 60200 Brno, Czech Republic. Tel: +420 541147234. Email: mica.l@fce.vutbr.cz.

REFERENCES

- Boháč, J. & Feda, J. 1995. Chování rozpukaných třetihorních jílu. In Proc. Zakládání staveb, Brno, November 1995. Sekurkon: 168-173. (in Czech)
- Boháč, J. 1999. Pevnost a přetváření brněnského jílu (Strength and deformation of Brno clay), In Proc. 11th International scientific conference, section Geotechnics, Brno, 18-20 October 1999. Akademické nakladatelství CERM Brno: 33-36. (in Czech)
- Erbenová, A. 2006. Faktory ovlivňující mechanické chování jílovitých zemin. Doctor thesis, Brno University of Technology, Faculty of Civil Engineering. (in Czech)
- Horák, V. 1987. Brno – kolektor Gottwaldova – šachta 15A, geotechnický sled. Research report, Geotest Brno, arch. č. 86 0628. (in Czech)
- Penman, J. (1998). User's manual – version 6.03, WinWall – The Tensar reinforced retaining wall design program, Appendix D
- Rowe, R.K. & Skinner, G.D. (2001). Numerical analysis of geosynthetics reinforced retaining wall constructed on layered soil foundation, Geotextiles and Geomebranes, 19, No. 7, 387-412
- Schanz, T., Vermeer, P.A. & Bonnier, P.G. (1999). The hardening soil model: Formulation and verification, In Proc. Beyond 2000 in Computational Geotechnics – 10 Years of Plaxis, Balkema: 168-173. (in Czech)
- Skinner, G.D. & Rowe, R.K. (2005). A novel approach to estimating the bearing capacity stability of geosynthetic reinforced retaining walls constructed on yielding foundations, Canadian Geotechnical Journal, 42, No. 3, 763-779
- Uhrin, M. 2004. Aplikace Cam Clay modelu na brněnský jíl – část "A": Zpráva. Diploma thesis, Brno University of Technology, Faculty of Civil Engineering. (in Czech)
- Vermeer, T. & Brinkgreve, R.B.J. (1998). Plaxis 2D: Finite element code for soil and rock analyses (Version 8.4), Balkema, Rotterdam
- Yoo, C. & Song, A.R. (2006). Effect of foundation yielding on performace of two-tier geosynthetics-reinforced segmental retaining walls: a numerical investigation, Geosynthetics International, 13, No. 5, 181-196